Atmos. Chem. Phys. Discuss., 8, 16851–16890, 2008
www.atmos-chem-phys-discuss.net/8/16851/2008/

Atmospheric Chemistry and Physics Discussions

This discussion paper is/has been under review for the journal *Atmospheric Chemistry and Physics (ACP)*. Please refer to the corresponding final paper in *ACP* if available.

Parameterization of cloud droplet formation for global and regional models: including adsorption activation from insoluble CCN

P. Kumar[1], **I. N. Sokolik**[2], **and A. Nenes**[1,2]

[1]School of Chemical and Biomolecular Engineering, Georgia Institute of Technology, Atlanta, GA, USA
[2]School of Earth and Atmospheric Sciences, Georgia Institute of Technology, Atlanta, GA, USA

Received: 22 July 2008 – Accepted: 9 August 2008 – Published: 8 September 2008

Correspondence to: A. Nenes (nenes@eas.gatech.edu)

Published by Copernicus Publications on behalf of the European Geosciences Union.

Abstract

Dust and black carbon aerosol have long been known to have potentially important and diverse impacts on cloud droplet formation. Most studies to date focus on the soluble fraction of such particles, and ignore interactions of the insoluble fraction with water vapor (even if known to be hydrophilic). To address this gap, we develop a new parameterization framework that considers cloud droplet formation within an ascending air parcel containing insoluble (but wettable) particles mixed with aerosol containing an appreciable soluble fraction. Activation of particles with a soluble fraction is described through well-established Köhler Theory, while the activation of hydrophilic insoluble particles is treated by "adsorption-activation" theory. In the latter, water vapor is adsorbed onto insoluble particles, the activity of which is described by a multilayer Frankel-Halsey-Hill (FHH) adsorption isotherm modified to account for particle curvature. We further develop FHH activation theory, and i) find combinations of the adsorption parameters A_{FHH}, B_{FHH} for which activation into cloud droplets is not possible, and, ii) express activation properties (critical supersaturation) that follow a simple power law with respect to dry particle diameter.

Parameterization formulations are developed for sectional and lognormal aerosol size distribution functions. The new parameterization is tested by comparing the parameterized cloud droplet number concentration against predictions with a detailed numerical cloud model, considering a wide range of particle populations, cloud updraft conditions, water vapor condensation coefficient and FHH adsorption isotherm characteristics. The agreement between parameterization and parcel model is excellent, with an average error of 10% and R^2~0.98.

1 Introduction

It is well established that atmospheric aerosols are often hydrophilic, and can serve as Cloud Condensation Nuclei (CCN), upon which cloud droplets are formed through the

ACPD

8, 16851–16890, 2008

process of activation. Changes in CCN concentration affect the radiative properties of clouds, known as the "first aerosol indirect" or "Twomey" effect (Twomey, 1974). The enhanced number of droplets is often accompanied by a reduction in their size, there by affecting cloud precipitation efficiency. This may result in increased cloudiness, which gives rise to the so called "second aerosol" or "Albrecht" effect (Albrecht, 1989). Through their interactions with clouds, tropospheric aerosols play an important role in changing the Earth's radiative budget, being one of the most uncertain components of climate change (IPCC 2007).

Cloud droplet activation is the direct microphysical link between aerosols and clouds, and is at the heart of the indirect effect (Nenes and Seinfeld, 2003). Droplet activation in atmospheric models is calculated from parameterizations whose sophistication ranges from empirical correlations (relating aerosol mass or number concentration to cloud droplet number concentration) to physically-based prognostic formulations (Feingold and Heymsfield, 1992; Boucher and Lohmann, 1995; Gultepe and Isaac, 1996; Abdul-Razzak et al., 1998; Abdul Razzak and Ghan, 2000; Cohard et al., 2000; Nenes and Seinfeld, 2003; Fountoukis and Nenes, 2005; Ming et al., 2006; Barahona and Nenes, 2007). All parameterizations developed to date rely on Köhler theory (Köhler, 1936), which considers curvature and solute effects on the equilibrium vapor pressure of a growing droplet. Most often, this equilibrium curve exhibits a maximum in supersaturation, known as critical supersaturation, s_c, at the critical wet droplet diameter, D_c. According to Köhler theory, when a particle is exposed to saturation above s_c for long enough to exceed D_c, it is in unstable equilibrium and can nucleate a cloud droplet.

Insoluble atmospheric particles, like mineral dust and soot, can also act as efficient cloud condensation nuclei (e.g. Seisel et al., 2005), if they acquire some amount of deliquescent materials (like $(NH_4)_2SO_4$)). The threshold of nucleation substantially decreases when water interacts (adsorbs) onto slightly soluble particles giving rise to the process of adsorption activation (Sorjamma and Laaksonen, 2007; Henson, 2007). Henson (2007) showed that a number of existing adsorption models (e.g., Fletcher, 1958; Wexler and Ge, 1998) for slightly soluble and insoluble particles can be suc-

cessfully applied to represent droplet formation from adsorption activation. Similarly, Sorjamma and Laaksonen (2007) used the Frankel-Halsey-Hill (FHH) multilayer physical adsorption model to describe water uptake as a function of relative humidity (i.e., water activity) and applied the theory to describe the activation of insoluble hydrophilic CCN. As with Köhler theory, resulting equilibrium curves of Henson (2007) and Sorjamma and Laaksonen (2007) exhibit a critical supersaturation that characterizes the minimum level of s required for a particle to act as a CCN.

To date, there is no parameterization framework that can concurrently treat the competition of insoluble and soluble CCN in the cloud droplet formation process; this gap is addressed in this study. This new activation parameterization builds upon the frameworks of Nenes and Seinfeld (2003), Fountoukis and Nenes (2005) and Barahona and Nenes (2007) to include effects of adsorption activation, based on the formulation of Sorjamma and Laaksonen (2007). The insoluble particles (referred to in this study as FHH particles) are considered to be externally mixed with hydrophilic deliquescent particles (referred to as Köhler particles) all of which compete for water vapor in a cloud updraft, thus allowing for the comprehensive treatment of kinetic limitations, chemical effects (i.e., slow water vapor condensation and surface tension depression) and entrainment effects on cloud droplet formation.

A brief discussion of FHH adsorption activation and Köhler theory is given in Sect. 2. Section 3 describes the formulation of the new parameterization for sectional and lognormal representation of size distribution. An evaluation of the parameterization by comparing against predictions of a numerical cloud parcel model is done in Sect. 4. Finally, a summary is presented in Sect. 5.

2 Theory of adsorption activation

A number of adsorption isotherm models exist to describe the process of physisorption of gas-phase species onto solid surfaces, such as Langmuir (Langmuir, 1916), BET (Brunauer, Emmet and Taylor) (Brunauer et al., 1938), and FHH (Frenkel, Halsey

and Hill) isotherms. The Langmuir isotherm is the first and perhaps the most studied adsorption model developed until to date. However, it is limited to describing the adsorption of a monolayer of water vapor, and hence it is not applicable to atmospheric particles, where the vapor pressure is high enough to form multiple layers of water vapor adsorbed onto the CCN. BET and FHH adsorption isotherm models were developed to treat multilayer adsorption, and have been explored to study adsorption activation, or, the process of cloud droplet formation from adsorption of water vapor onto insoluble particles (e.g., Henson, 2007; Sorjamma and Laaksonen, 2007).

2.1 FHH adsorption theory

In this study, we use the FHH adsorption theory (Sorjamma and Laaksonen, 2007) to describe the process of adsorption activation in which the water vapor saturation ratio, S, of a particle in equilibrium with surrounding water vapor can be expressed as

$$S = \alpha_w \exp\left(\frac{4\sigma M_w}{RT\rho_w D_p}\right) \quad (1)$$

where α_w is the activity of the water in the particle, σ is the surface tension at the particle-gas interface, M_w is the molar mass of water, R is the universal gas constant, T is the temperature, ρ_w is the density of water, and D_p is the particle diameter. The exponential in Eq. (1) is commonly referred to as the curvature, or Kelvin effect. According to FHH theory, $\alpha_w = \exp(-A_{\mathrm{FHH}}\Theta^{-B_{\mathrm{FHH}}})$ (Sorjamma and Laaksonen, 2007); substitution in Eq. (1) then gives

$$S = \exp\left(\frac{4\sigma M_w}{RT\rho_w D_p}\right)\exp(-A_{\mathrm{FHH}}\Theta^{-B_{\mathrm{FHH}}}) \quad (2)$$

where A_{FHH}, B_{FHH} are empirical constants, and Θ is the surface coverage (defined as the number of adsorbed water molecules divided by the number of molecules in a monolayer). A_{FHH} characterizes interactions of adsorbed molecules with the aerosol

surface and adjacent adsorbate molecules (i.e., those in the first monolayer). B_{FHH} characterizes the attraction between the aerosol surface and the adsorbate in subsequent layers; the smaller the value of B_{FHH}, the greater the distance at which the attractive forces act (Sorjamma and Laaksonen, 2007). A_{FHH} and B_{FHH} are compound-specific and determined experimentally. It has been found experimentally that A_{FHH} ranges from 0.1 to 3.0 while the value of B_{FHH} ranges from 0.5 to 3.0 (Sorjamma and Laaksonen, 2007).

Equation (2) expresses S in terms of two spatial scales, D_p and Θ. However, Θ can be expressed in terms of D_{dry} as (Sorjamma and Laaksonen, 2007):

$$\Theta = \frac{D_p - D_{dry}}{2D_w} \tag{3}$$

where D_{dry} is the dry particle diameter and D_w is the diameter of a water molecule adsorbed on the particle surface. Substituting Eq. (3) into Eq. (2), expressed in terms of equilibrium supersaturation $s = S - 1$, gives an equation that depends only on D_p,

$$s = \exp\left[\frac{4\sigma M_w}{RT\rho_w D_p} - A_{FHH}\left(\frac{D_p - D_{dry}}{2D_w}\right)^{-B_{FHH}}\right] - 1 \cong \frac{4\sigma M_w}{RT\rho_w D_p} - A_{FHH}\left(\frac{D_p - D_{dry}}{2D_w}\right)^{-B_{FHH}} \tag{4}$$

The activation behavior of particles following FHH theory can be rationalized by analyzing the derivative of s with respect to D_p:

$$\frac{ds}{dD_p} = \left(-\frac{4\sigma M_w}{RT\rho_w D_p^2}\right) + \left(\frac{A_{FHH}B_{FHH}}{2D_w}\left(\frac{D_p - D_{dry}}{2D_w}\right)^{-B_{FHH}-1}\right) \tag{5}$$

where the first and second terms in the right hand side of Eq. (5) correspond to the contribution due to Kelvin effect and adsorption effect, respectively. If B_{FHH} is large enough, both terms in Eq. (5) can become equal for a characteristic wet diameter, D_c, so that $\left.\frac{ds}{dD_p}\right|_{D_p=D_c} = 0$. Under such conditions, FHH particles behave much like those following

ACPD
8, 16851–16890, 2008

Köhler theory, with s becoming maximum (known as critical supersaturation, s_c) at the critical wet diameter D_c. s_c is determined by solving $\frac{ds}{dD_p}=0$ so Eq. (5) becomes

$$\left(-\frac{4\sigma M_w}{RT\rho_w D_c^2}\right)+\left(\frac{A_{\mathrm{FHH}}B_{\mathrm{FHH}}}{2D_w}\left(\frac{D_c-D_{\mathrm{dry}}}{2D_w}\right)^{-B_{\mathrm{FHH}}-1}\right)=0 \quad (6)$$

Numerically solving Eq. (6) gives D_c, which can then be substituted in Eq. (4) to obtain s_c. If B_{FHH} is small enough so that $\left(-\frac{4\sigma M_w}{RT\rho_w D_p^2}\right) << \left(\frac{A_{\mathrm{FHH}}B_{\mathrm{FHH}}}{2D_w}\left(\frac{D_p-D_{\mathrm{dry}}}{2D_w}\right)^{-B_{\mathrm{FHH}}-1}\right)$ for all values of D_p, then the equilibrium curve is dominated by the adsorption term and the particle is always in stable equilibrium with the environment, i.e., the particles never activate into cloud droplets.

2.2 Activation characteristics of FHH and Köhler particles

It is important to know which combinations of A_{FHH} and B_{FHH} give equilibrium curves with a maximum and can therefore act as CCN. This is done by determining the range of A_{FHH}, B_{FHH} and D_{dry} for which a solution to Eq. (6) exists, for the reported range for A_{FHH} and B_{FHH} (0.1–3.0 and 0.5–3.0, respectively; Sorjamma and Laaksonen, 2007), and, D_{dry} between 0.03 μm and 150 μm. When a solution for D_c is found, we normalize it with D_{dry} to express the growth required by FHH particles to activate.

Figure 1 shows contour plots of D_c/D_{dry} for the D_{dry} equal to 0.25 μm and 20 μm. For B_{FHH}<0.7–0.8 and any value of A_{FHH} (area filled with purple color), D_c could not be found. Conversely, for B_{FHH}>0.9 and any given value of A_{FHH}, a solution for D_c always exists. Since the contour plots for different dry particle diameters are very similar, this suggests that D_c/D_{dry} has a weak dependence on D_{dry}. Furthermore, for most combinations of A_{FHH} and B_{FHH}, the value of D_c/D_{dry} lies between 1–2, which suggests that D_c is very close to D_{dry}, i.e., the amount of water required to activate FHH particles is small. This is an important finding that facilitates the computation of

ACPD
8, 16851–16890, 2008

the condensation integral (required by the parameterization, see Sect. 3.6).

The activation of particles containing soluble material is described by Köhler theory (Köhler, 1936; Seinfeld and Pandis, 1998) in which equilibrium supersaturation is given by

$$s = \frac{A}{D_p} - \frac{B}{D_p^3} \tag{7}$$

where $A = \frac{4M_w\sigma}{RT\rho_w}$ and $B = \frac{6n_sM_wv}{\pi\rho_w}$. Here n_s are the moles of solute in the particle and v is the effective van't Hoff factor of the solute. The s_c and D_c for Köhler particles are then given by:

$$s_c = \left(\frac{4A^3}{27B}\right)^{1/2} \tag{8a}$$

$$D_c = \left(\frac{3B}{A}\right)^{1/2} \tag{8b}$$

3 Formulation of parameterizations for Köhler and FHH theories

The aerosol activation parameterization is based on the cloud parcel framework, in which a parcel of air containing a mixture of Köhler particles (i.e., particles consisting of water-soluble species) and FHH particles (water insoluble species) is lifted and cooled. When supersaturation develops, droplets begin forming (by the process of activation) up to the point where supersaturation in the parcel reaches a maximum, $s_{\max}$. If the CCN spectrum (i.e., the number of CCN as a function of ambient supersaturation) and $s_{\max}$ are known, the droplet number, N_d, in the parcel can be computed as the number of CCN that activate at $s_{\max}$. The new parameterization determines both $s_{\max}$ and N_d. Since sectional and lognormal representations of the aerosol particle size distribution are most frequently used in the models, we develop formulations for both.

ACPD
8, 16851–16890, 2008

3.1 Sectional representation of CCN spectrum

The sectional representation uses discrete size classes (bins or sections) for the aerosol distribution. Each section can have its own chemical composition. If the aerosol mixture is composed of k populations (i.e., aerosol types), then a separate binning is assigned to each type. The cumulative size distribution is then determined by summing over all the populations (Nenes and Seinfeld, 2003):

$$F^d(d) = \sum_{l=1}^{k} \int_0^d n_l^d(D_p')d(D_p') = \sum_{l=1}^{k} \left[\sum_{j=1}^{m(l)-1} N_{j,l} + N_{m(l),l} \left(\frac{d - D_{p,m(l)-1}^l}{D_{p,m(l)}^l - D_{p,m(l)-1}^l} \right) \right] \quad (9)$$

where m is the section of population l that contains particles of size d with bin size limits $D_{p,m(l)-1}^l$ and $D_{p,m(l)}^l$, and $N_{m(l),l}$ is the aerosol number concentration of section m.

The aerosol critical supersaturation distribution function, $n_l^s(s)$, is then determined by mapping the aerosol particle size distribution onto supersaturation coordinates (Nenes and Seinfeld, 2003),

$$n_l^s(s) = \frac{dN}{ds} = \sum_{l=1}^{k} \frac{N_{i(l),l}}{s_{c,i(l)} - s_{c,i(l)-1}}, \quad s_{c,i(l)-1} \le s \le s_{c,i(l)} \quad (10)$$

where $s_{c,i(l)}$ and $s_{c,i(l)-1}$ are the critical supersaturations corresponding to the boundaries of section i and population l, and $N_{i(l),l}$ is the concentration of CCN between $s_{c,i(l)}$ and $s_{c,i(l)+1}$. The CCN spectrum, $F^s(s)$, is then obtained by integration of $n^s(s)$ from 0 to s:

$$F^s(s) = \sum_{l=1}^{k} \int_0^s n_l^s(s')ds' = \sum_{l=1}^{k} \left[\sum_{j=1}^{i(l)-1} N_{j,l} + N_{i(l),l} \left(\frac{s - s_{c,i(l)-1}^l}{s_{c,i(l)}^l - s_{c,i(l)-1}^l} \right) \right] \quad (11)$$

ACPD
8, 16851–16890, 2008

The relationship between $s^{l}_{c,i(l)}$ and $d^{l}_{p,m(l)}$ depends on the theory used for describing activation. For Köhler particles, Eq. (8a) is used, while for FHH particles, the procedure outlined in Sect. 2.1 is used.

3.2 Lognormal representation of CCN spectrum

A lognormal distribution is often expressed as

$$\frac{dN}{d\ln D_{\text{dry}}} = \sum_{i=1}^{n_m} \frac{N_i}{\sqrt{2\pi}\ln\sigma_i} \exp\left[-\frac{\ln^2(D_{\text{dry}}/D_{g,i})}{2\ln^2\sigma_i}\right] \tag{12}$$

where σ_i and $D_{g,i}$ are the geometric standard deviation and median diameter, respectively, for the ith lognormal mode, and n_m is the number of lognormal modes in the size distribution. Assuming each mode (or population) has uniform chemical composition, a power law function can be used to express $D_{\text{dry}}/D_{g,i}$ in terms of a critical supersaturation ratio, $s/s_{g,i}$,

$$\frac{D_{\text{dry}}}{D_{g,i}} = \left[\frac{s}{s_{g,i}}\right]^{\frac{1}{x}} \tag{13}$$

where s and $s_{g,i}$ are critical supersaturations of CCN with dry diameter D_{dry} and $D_{g,i}$ respectively, and x is an exponent that depends on the activation theory used. For particles following Köhler theory, $x=-3/2$, while for FHH particles, x depends on A_{FHH} and B_{FHH} (see Sect. 3.3).

The aerosol critical supersaturation distribution function, $n^{s}(s)$, can then be calculated as follows (Fountoukis and Nenes, 2005)

$$n^{s}(s) = \frac{dN}{ds} = -\frac{dN}{d\ln D_{\text{dry}}}\cdot\frac{d\ln D_{\text{dry}}}{ds} \tag{14}$$

ACPD
8, 16851–16890, 2008

where the negative sign has been applied to reflect that $dD_p = -ds$. Substituting $D_{\mathrm{dry}}/D_{g,i}$ from Eq. (13) into Eq. (12) gives

$$\frac{dN}{d\ln D_{\mathrm{dry}}} = \sum_{i=1}^{n_m} \frac{N_i}{\sqrt{2\pi}\ln\sigma_i} \exp\left[-\frac{\ln^2(s/s_{g,i})^{\frac{1}{x}}}{2\ln^2\sigma_i}\right] \tag{15}$$

Differentiating Eq. (13) also gives

$$\frac{d\ln D_{\mathrm{dry}}}{ds} = \frac{1}{xs} \tag{16}$$

Substituting Eqs. (16) and (15) into Eq. (14) gives

$$n^s(s) = \sum_{i=1}^{n_m} -\frac{N_i}{\sqrt{2\pi}\ln\sigma_i}\frac{1}{xs} \exp\left[-\frac{\ln^2(s/s_{g,i})^{\frac{1}{x}}}{2\ln^2\sigma_i}\right] \tag{17}$$

The CCN spectrum, $F^s(s)$, is then obtained by integration of $n^s(s)$ from 0 to s:

$$F^s(s) = \int_0^s n^s(s')ds' = \sum_{i=1}^{n_m} \frac{N_i}{2}\mathrm{erfc}\left[-\frac{\ln(s_{g,i}/s)}{x\sqrt{2}\ln\sigma_i}\right] \tag{18}$$

Equation (18) is the generalized form of a CCN spectrum for the lognormal particle size distribution, and the value of x encompasses the physics behind the aerosol-water vapor interaction (i.e., Köhler or FHH). For $x=-3/2$ (Köhler particles), Eq. (18) reduces to the formulation given by Fountoukis and Nenes (2005):

$$F^s(s) = \int_0^s n^s(s')ds' = \sum_{i=1}^{n_m} \frac{N_i}{2}\mathrm{erfc}\left[\frac{2\ln(s_{g,i}/s)}{3\sqrt{2}\ln\sigma_i}\right] \tag{19}$$

3.3 Exponent x for FHH particles

In determining the value of x in Eq. (13) for FHH particles, we computed numerically the ratio of $s/s_{g,i}$ (using the procedure in Sect. 2.1) for a wide range of $D_{g,i}$ (0.03 μm–0.1 μm), D_{dry} (0.05 μm–0.8 μm), and A_{FHH} and B_{FHH} (8 different combinations as shown in Table 3). As can be seen in Fig. 2, for given values of A_{FHH} and B_{FHH}, $s/s_{g,i}$and $D_{\mathrm{dry}}/D_{g,i}$, exhibit a power-law dependence. This dependence holds for the entire range of $D_{g,i}$ and D_{dry} considered. Power law fits to these calculations can then be used to describe x as a function of A_{FHH} and B_{FHH}. The results are shown in Fig. 3. For each A_{FHH}, x has a maximum at B_{FHH}~1.3, while x is always negative, varying between −1.0 to −0.8, depending on the value of A_{FHH}.

Multivariate least squares regression was performed on the data of Fig. 3 to determine an analytical relationship between x and, A_{FHH} and B_{FHH}:

$$x = \sum_{i=1}^{4} \frac{C_i}{B_{\mathrm{FHH}}^{i-1}} \tag{20}$$

where C_i is given by,

$$C_i = \sum_{j=1}^{5} \frac{D_{j,i}}{A_{\mathrm{FHH}}^{j-1}} \tag{21}$$

$D_{j,i}$ are fitting parameters, and are given in Table 2. Using Eq. (21), the data in Fig. 3 can be reproduced with an average relative error of 0.5%±1%.

Equation (13) suggests that s_c of FHH particles can be written as $s_c = C D_{\mathrm{dry}}^{x}$, where C is a constant that depends on A_{FHH} and B_{FHH}. C can be determined by computing s_c (Sect. 2.1) for a reference dry diameter. Figure 4 presents C as a function of A_{FHH} and B_{FHH}, computed for particles of 0.1 μm dry diameter.

ACPD
8, 16851–16890, 2008

3.4 Computation of s_{max} and N_d

The s_{max} in a cloud corresponds to the point where supersaturation generation from cooling balances depletion from condensation of water vapor, and characterizes the point where droplet activation terminates. For a non-adiabatic (entraining) cloud parcel ascending with constant velocity V, s_{max} can be determined from the solution of the following equation (Barahona and Nenes, 2007)

$$\frac{2\alpha V}{\pi\gamma\rho_w} - Gs_{max}\int_0^{s_{max}}\left(D_p^2(\tau)+2G\int_\tau^{t_{max}}\mathrm{sdt}\right)^{1/2} n^s(s')ds'=0 \quad (22)$$

where $D_p(\tau)$ is the size of CCN when exposed to $s=s_c$, $\gamma=\frac{pM_a}{p^sM_w}+\frac{M_w\Delta H_v^2}{c_pRT^2}$, $\alpha=\frac{gM_w\Delta H_v}{c_pRT^2}-\frac{gM_a}{RT}+e\left[\frac{\Delta H_vM_w}{RT^2}(T-T')-(1-\mathrm{RH})\right]$, ΔH_v is the latent heat of condensation of water, g is the acceleration due to gravity, T is the temperature of the parcel, M_w is the molecular weight of water, M_a is the molecular weight of air, c_p is the heat capacity of air, p^s is the water saturation vapor pressure, p is the ambient pressure, e is the entrainment rate of dry air into the parcel (m^{-1}), and T, and RH are the ambient temperature and fractional relative humidity, respectively. G in Eq. (22) is given by

$$G=\frac{4}{\frac{\rho_wRT}{p^sD_{v'}M_w}+\frac{\Delta H\rho_w}{k_aT}\left(\frac{\Delta H_vM_w}{RT}-1\right)} \quad (23)$$

where k_a is the thermal conductivity of air, and $D_{v'}$ is the water vapor mass transfer coefficient from the gas to droplet phase corrected for non-continuum effects that is calculated as discussed in Sect. 3.5. For an adiabatically rising parcel, e=0, and hence Eq. (22) can be re-written as,

$$\frac{2\alpha V}{\pi\gamma\rho_w} - I_e(0, s_{max})=0 \quad (24)$$

ACPD
8, 16851–16890, 2008

where

$$I_e(0, s_{\max}) = G s_{\max} \int_0^{s_{\max}} \left(D_p^2(\tau) + 2G \int_\tau^{t_{\max}} \mathrm{sdt} \right)^{1/2} n^s(s') ds' \quad (25)$$

$I_e(0, s_{\max})$ is called the condensation integral (further treated in Sect. 3.6), which upon calculation can be substituted in Eq. (24) and subsequently solved for $s_{\max}$. Then, the number of cloud droplets that form in the parcel is

$$N_d = F^s(s_{\max}) \quad (26)$$

3.5 Accounting for size and compositional effects on mass transfer coefficient

It is well known that the mass transfer coefficient of water vapor onto droplets (otherwise known as the effective diffusivity), D_v', varies with particle size (Fukuta and Walter, 1970),

$$D_v' = \frac{D_v}{1 + \frac{2D_v}{\alpha_c D_p}\sqrt{\frac{2\pi M_w}{RT}}} \quad (27)$$

where D_v' is the water vapor diffusivity in air, and α_c is the water vapor uptake coefficient. The α_c is a kinetic parameter, expressing the probability of water vapor molecules of being incorporated into droplet upon collision. However, processes other than accommodation can control the condensation of water vapor (e.g., dissolution kinetics, Asa-Awuku and Nenes, 2007). Thus, α_c can be used to express collectively all related processes in terms of an effective uptake coefficient. Neglecting to account for the size dependency in D_v' results in overestimating water vapor condensation in the initial stages of cloud formation (Feingold and Chuang, 2002; Nenes et al., 2002; Ming et al., 2006; Fountoukis and Nenes, 2007), which can lead to an underestimation of $s_{\max}$ and N_d.

An analytical form of the condensation integral cannot be derived by substituting Eq. (27) into Eq. (25). Instead, Fountoukis and Nenes (2005) suggested to use an average mass transfer coefficient, $D_{v,\mathrm{ave}}$, for the growing droplet population. Assuming that α_c is constant for all CCN, and $D_{p,\mathrm{low}}$ and $D_{p,\mathrm{big}}$ express the upper and lower size of droplets responsible for the condensation of water vapor (hence mass transfer), $D_{v,\mathrm{ave}}$ can be expressed as (Fountoukis and Nenes, 2005):

$$D_{v,\mathrm{ave}} = \frac{D_v}{D_{p,\mathrm{big}} - D_{p,\mathrm{low}}} \left[\left(D_{p,\mathrm{big}} - D_{p,\mathrm{low}} \right) - B' \ln \left(\frac{D_{p,\mathrm{big}} + B'}{D_{p,\mathrm{low}} + B'} \right) \right] \tag{28}$$

where $B' = \frac{2D_v}{\alpha_c} \left(\frac{2\pi M_w}{RT} \right)^{1/2}$. Based on numerical simulations for a wide range of values of involved parameters, Fountoukis and Nenes (2005) suggest $D_{p,\mathrm{big}} = 5\,\mu\mathrm{m}$ and $D_{p,\mathrm{low}} = \min\{0.207683\alpha_c{}^{-0.33048}, 5.0\}$.

3.6 Computing the condensation integral $I_e(0, s_{\max})$

To compute the condensation integral (Eq. 25), we first express it as the sum of two terms. The first one gives the contribution from particles that follow Köhler theory, $I_K(0, s_{\max})$, whereas the second one from FHH particles, $I_{\mathrm{FHH}}(0, s_{\max})$:

$$I_e(0, s_{\max}) = I_K(0, s_{\max}) + I_{\mathrm{FHH}}(0, s_{\max}) \tag{29}$$

Using the population splitting approach of Nenes and Seinfeld (2003), $I_K(0, s_{\max})$ is calculated as:

$$I_K(0, s_{\max}) = I_{K,1}(0, s_{\mathrm{part}}) + I_{K,2}(s_{\mathrm{part}}, s_{\max}) \tag{30}$$

where $I_{K,1}(0, s_{\mathrm{part}})$ corresponds to Köhler CCN that, at the instant of parcel maximum supersaturation, either do not strictly activate ($D_p \ll D_c$), or experience significant growth beyond their critical diameter ($D_p \gg D_c$). The $I_{K,2}(s_{\mathrm{part}}, s_{\max})$ corresponds to CCN that have not grown significantly beyond their critical diameter and for which

ACPD
8, 16851–16890, 2008

$D_p^2(\tau) >> 2G \int_{\tau}^{t_{max}} sdt$ (Nenes and Seinfeld, 2003). Calculations of the partitioning supersaturation, s_{part}, and $I_{K,1}(0, s_{part})$ and $I_{K,2}(s_{part}, s_{max})$ for sectional and lognormal size distribution formulations are presented in detail by Nenes and Seinfeld (2003), Fountoukis and Nenes (2005), and Barahona and Nenes (2007), and are not repeated here.

$I_{FHH}(0, s_{max})$ in Eq. (29) represents the contribution of FHH particles to the condensation integral. According to Sect. 2.2, $D_c/D_{dry} \sim 1$ for most values of A_{FHH} and B_{FHH}, and is much smaller that (D_c/D_{dry}) for Köhler particles with similar dry diameters. Compared to FHH particles, Köhler particles may require 8 to 1500 times more water (i.e., 2 to 50 times more in diameter) to become activated (Table 1). This means that $D_p \gg D_c$ can be assumed for all FHH particles. Hence, $D_p^2(\tau) << 2G \int_{\tau}^{t_{max}} sdt$ and the corresponding condensation integral is

$$I_{FHH}(0, s_{max}) = G s_{max} \int_0^{s_{max}} \left(2G \int_{\tau}^{t_{max}} sdt \right)^{1/2} n^s(s')ds' \approx G s_{max} \int_0^{s_{max}} \left(2G \frac{1}{2\alpha V} \left(s_{max}^2 - s'^2 \right) \right)^{1/2} n^s(s')ds' \quad (31)$$

where $\int_{\tau}^{t_{max}} sdt$ in Eq. (31) is evaluated using the lower bound of Twomey (1959) (Nenes and Seinfeld, 2003).

For sectional representation of aerosol size distributions, $I_{FHH}(0, s_{max})$ is computed by substituting Eq. (11) into Eq. (31), and performing the integration as follows

$$I_{FHH}(0, s_{max}) = \left(\frac{G}{\alpha V} \right)^{1/2} \sum_{j=1}^{i_{max}} \frac{N_j}{s_c^j - s_c^{j-1}} \left[\frac{x}{2} \left(s_{max}^2 - x^2 \right)^{1/2} + \frac{s_{max}^2}{2} \arcsin \frac{x}{s_{max}} \right]_{x=s_c^{j-1}}^{x=s_c^j} \quad (32)$$

where i_{max} is the boundary closest to s_{max}.

ACPD
8, 16851–16890, 2008

For lognormal representation of aerosol size distribution, $I_{FHH}(0, s_{max})$ is computed by substituting Eq. (17) into Eq. (31), and integrating

$$I_{FHH}(0, s_{max}) = \left(\frac{G}{\alpha V}\right)^{1/2} \frac{N_i s_{max}}{2} \left[1 - \left(\frac{s_{g,i}}{s_{max}}\right)^2 \exp(2x^2 \ln^2 \sigma_i) \frac{\left(\text{erf}(\sqrt{2}x\sigma_i - u_{max}) + 1\right)}{2} - \text{erf}(u_{max})\right] \quad (33)$$

where $u_{max} = \frac{\ln(s_{g,i}/s_{max})^{-\frac{1}{x}}}{\sqrt{2}\ln\sigma_i}$. In the case of multiple lognormal modes, Eq. (33) contains the sum of contributions from each mode.

3.7 Using the parameterization

The parameterization algorithm is illustrated in Fig. 5, and consists of two steps. First, Eq. (24) is numerically solved for s_{max} using the bisection method:

$$\frac{\pi\gamma\rho_w G s_{max}}{2\alpha V}\left[I_{K,1}(0, s_{part}) + I_{K,2}(s_{part}, s_{max}) + I_{FHH}(0, s_{max})\right] - 1 = 0 \quad (34)$$

where the condensation integral is substituted with the desirable formulation (sectional or lognormal). Physical properties are evaluated at the cloud base conditions for adiabatic updrafts (i.e., e=0). For entraining parcels (i.e., e>0), properties are evaluated at the critical entrainment rate following the procedure of Barahona and Nenes (2007). Once s_{max} is determined, N_d is obtained from Eq. (26).

4 Evaluation of the parameterization

4.1 Method

We first test the sectional formulation against the lognormal formulation to show the consistency between the two formulations. Then, we evaluate the accuracy of the parameterization by comparing the predicted droplet number concentration and maximum

supersaturation against the numerical parcel model of Nenes at al. (2001) (modified to include FHH particles) for a wide range of size distributions representative of global aerosols.

4.2 Evaluation of involved parameters

Nenes and Seinfeld (2003), Fountoukis and Nenes (2005) and Barahona and Nenes (2007) have extensively evaluated the parameterization for aerosol composed of only Köhler particles. Therefore, the focus of this evaluation is on the performance of the parameterization when FHH particles are mixed with Köhler particles, considering a wide range of FHH parameters (A_{FHH} and B_{FHH}), water vapor accommodation coefficient, α_c, and parcel updraft velocity, V. The values of α_c and V were selected to represent typical conditions encountered in low-level cumulus and stratocumulus clouds of marine and continental origin (Pontikis et al., 1987; Conant et al., 2004; Meskhidze et al., 2005; Peng et al., 2005; Barahona and Nenes, 2007). In total, 6400 different sets of conditions were considered (see Table 3).

A_{FHH} was varied between 0.5 to 2.0 while B_{FHH} from 0.93 to 2.0. The parcel pressure and temperature were 1.013 kPa and 290 K, respectively, and droplet concentration was taken at 350 m above the cloud base. For this comparison, we selected four Whitby (1978) trimodal size distributions, namely marine, clean continental, average background, and urban (Table 4). We also selected four additional aerosol distributions that are representative of dust (Jeong and Sokolik, 2007). They are C04 (Clarke et al., 2004), D87 (D'Almeida, 1987), O98 (Hess et al., 1998), and W08 (Weigner et al., 2008), the properties of which are given in Table 5. As expected, the distributions given by Whitby have smaller median diameters in comparison to those for distributions representative of dust. For each aerosol size distribution, we consider a mixture of Köhler and FHH particles, allowing the proportion to vary from 0% (pure Köhler particles) to 100% (pure FHH particles) by number.

ACPD
8, 16851–16890, 2008

4.3 Comparison of sectional against lognormal formulation

The sectional formulation is evaluated against the lognormal formulation by comparing N_d predicted by the application of each formulation to the activation of lognormal aerosol size distributions shown in Tables 4 and 5. In applying the sectional formulation, 75 sections per mode were used to discretize the lognormal distribution. The intercomparison is shown in Fig. 6, which depicts the parameterized N_d using the sectional versus the lognormal formulation. Whitby (1974) aerosol size distributions, α_c=0.042, A_{FHH} equal to 0.68, and B_{FHH} equal to 0.93 were used in the comparison. An excellent agreement between the two formulations is obtained for all cases considered (R^2=0.9998), suggesting both formulations are equivalent.

4.4 Comparison of sectional parameterization with parcel model

4.4.1 Whitby aerosol distribution

Figure 7 shows that the predicted droplet number from parameterization closely follows the predicted droplet number from the parcel model for all conditions of Table 3, thus indicating that there are no regions with systematic biases in the predictions (average relative error 0.37%±16%). Figure 8 shows the comparison for the predicted droplet number between the parameterization and the parcel model for individual Whitby (1978) distributions. An excellent agreement is apparent, with an average error of less than 10% (Table 6). The only exception is the case of the marine aerosol size distribution, where a systematic overprediction in parameterized N_d is observed. According to Barahona and Nenes (2007), this systematic bias results from an underestimation of the droplet size that causes a consequent underestimation of surface area available for water vapor condensation. This forces an underestimation of the condensation integral, thereby resulting in an overestimation in s_{max}, and hence N_d.

ACPD
8, 16851–16890, 2008

5 Dust size distributions

To test the applicability of this new parameterization to distributions representative of dust, we performed an extensive analysis on droplet number predictions comparisons between this parameterization and the parcel model on aerosol distributions suggested by Clarke et al. (2004), D'Almeida (1987), Hess et al. (1998) and Weigner et al. (2008) for the cloud conditions of Table 3.

Figure 9 shows a good agreement between parameterization and the parcel model for different updrafts and α_c=0.042, A_{FHH} equal to 0.68, and B_{FHH} equal to 0.93. The agreement is best at high updrafts (5 m s^{-1}, 10 m s^{-1}); at low updrafts (0.1 m s^{-1}, 0.5 m s^{-1}) overprediction by the parameterized N_d was observed. This is because of the overprediction in maximum parcel supersaturation, s_{max} (Fig. 10, right down), an explanation for which has been provided in the preceding Sect. 4.4.1. Figure 10 (left panels) shows droplet number concentration predictions for different dust distribution for all conditions of parcel updrafts, uptake coefficients, A_{FHH} equal to 0.68, and B_{FHH} equal to 0.93. The best performance is seen using the W08 (Weigner et al., 2008) dust distribution (Fig. 10c). This may be attributed to smaller median diameters for the Weigner et al. (2008) distribution in comparison to the much larger fraction of super-micron particles present in the Clarke et al. (2004), D'Almeida (1987), and Hess et al. (1998) distributions.

Figure 10 (right panels) compares parcel maximum supersaturation, s_{max}, between the parcel model and the parameterization for three different values of accommodation coefficients. At low values of α_c, a greater overprediction in s_{max} is observed. This consequently results in overprediction in the number of activated droplets, and manifests because of the underestimation of surface area available for water vapor condensation for the largest size of CCN as explained in Sect. 4.4.1. However, this overestimation in cloud droplet number becomes important only for very large values s_{max} that are not found in clouds.

ACPD
8, 16851–16890, 2008

6 Summary

This study presents a new parameterization of cloud droplet formation for an aerosol mixture consisting of soluble particles that activate according to Köhler theory, and completely insoluble particles that form droplets through adsorption activation following FHH adsorption theory. This new parameterization is the first of its kind and is built upon previous work of Nenes and Seinfeld (2003), Fountoukis and Nenes (2005), and Barahona and Nenes (2007).

Formulation of the parameterization is developed for sectional and lognormal representations of the aerosol size distribution. To facilitate the analytical development of the parameterization, we have further developed FHH activation theory by i) determining the range of A_{FHH} and B_{FHH} for which particles do not act as CCN, and, ii) linking critical superaturation with dry diameter using a simple power law expression, determined from numerical solutions to the FHH equilibrium curves.

The parameterization is tested by comparing predictions of droplet number and s_{max} against detailed cloud parcel model simulations. The evaluations are performed for a range of updraft velocities, water vapor uptake coefficients, ambient temperature, relative humidity, parameters of aerosol size distributions, and A_{FHH} and B_{FHH}. The parameterization closely follows the parcel model simulations with a mean relative error between 2% and 20%.

Future work is needed to experimentally derive appropriate values of A_{FHH} and B_{FHH} for dust, soot and other insoluble atmospheric particles. Once available, the framework presented here is uniquely placed for addressing questions related to the interactions of insoluble particles with clouds and climate.

Acknowledgements. This work was supported by NOAA ACC, NSF CAREER and NASA grants.

References

Abdul-Razzak, H. and Ghan, S.: A parameterization of aerosol activation – 2: Multiple aerosol types, J. Geophys. Res., 105(D6), 6837–6844, 2000.

Abdul-Razzak, H. and Ghan, S.: Parameterization of the influence of organic surfactants on aerosol activation, J. Geophys. Res., 109, D03205, doi:10.1029/2003JD004043, 2000.

Abdul-Razzak, H., Ghan, S., and Rivera-Carpio, C.: A parameterization of aerosol activation – 1: Single aerosol type, J. Geophys. Res., 103, 6123–6131, 2000.

Albrecht, B. A.: Aerosols, cloud microphysics, and fractional cloudiness, Science, 245, 1227–1230, 1989.

Barahona, D. and Nenes, A.: Parameterization of cloud droplet formation in large scale models: including effects of entrainment, J. Geophys. Res., 112, D16206, doi:10.1029/2007JD008473, 2007.

Boucher, O. and Lohmann, U.: The sulphate-CCN-cloud albedo effect: A sensitivity study with 2 general circulation models, Tellus B, 47, 281–300, 1995.

Brunauer, S., Emmett, P. H., and Teller, E.: Adsorption of gases in multimolecular layers, J. Am. Chem. Soc., 60(2), 309–319, 1938.

Clarke, A. D., Shinozuka, Y., Kapustin, V. N., Howell, S., Huebert, B., Doherty, S., Anderson, T., Covert, D., Anderson, J., Hua, X., Moore II, K. G., McNaughton, C., Carmichael, G., and Weber, R.: Size distributions and mixtures of dust and black carbon aerosol in Asian outflow: physiochemistry and optical properties, J. Geophys. Res., 109, D15S09, doi:10.1029/2003JD004378, 2004.

Cohard, J. M., Pinty, J. P., and Suhre, K.: On the parameterization of activation spectra from cloud condensation nuclei microphysical properties, J. Geophys. Res., 105(D9), 11 753–11 766, 2000.

Conant, W. C., Van Reken, T. M., Rissman, T. A., Varutbangkul, H., Jonsson, H. H., Nenes, A., Jimenez, J. L., Delia, A. E., Bahreini, R., Roberts, G. C., Flagan, R. C., and Seinfeld, J. H.: Aerosol-cloud drop concentration closure in warm cumulus, J. Geophys. Res., 109, D13204, doi:10.1029/2003JD004324, 2004.

D'Almeida, G. A.: On the variability of desert aerosol radiative characteristics, J. Geophys. Res., 92, 3017–3027, 1987.

Feingold, G. and Chuang, P. Y.: Analysis of influence of surface films on droplet growth: Implications for cloud microphysical processes and climate, J. Atmos. Sci., 59, 2006–2018,

2002.
Feingold, G. and Hymesfield, A. J.: Parameterization of condensational growth of droplets for use in general circulation models, J. Geophys. Res., 49, 2325–2342, 1992.
Fletcher, N. H.: Size effect in heterogeneous nucleation, J. Chem. Phys., 29, 572–576, 1958.
Fountoukis, C. and Nenes, A.: Continued development of a cloud droplet formation parameterization for global climate models, J. Geophys. Res., 110, D11212, doi:10.1029/2004JD005591, 2005.
Fukuta, N. and Walter, L. A.: Kinetics of hydrometer growth from the vapor; spherical model, J. Atmos. Sci., 27, 1160–1172, 1970.
Gultepe, I. and Isaac, G. A.: The relationship between cloud droplet and aerosol number concentrations for climate models, Int. J. Climatol., 16, 941–946, 1996.
Henson, B. F.: An adsorption model of insoluble particle activation: Application to black carbon, J. Geophys. Res., 112, D24S16, doi:10.1029/2007JD008549, 2007.
Hess, M., Koepke, P., and Schult, I.: Optical properties of aerosols and clouds: the software package OPAC, B. Am. Meteorol. Soc., 79, 831–844, 1998.
Intergovernmental Panel on Climate Change, Climate Change: the Scientific Basis, Cambridge University Press, Cambridge, UK, 2007.
Jeong, G. and Sokolik, I. N.: The effect of mineral dust aerosols on photolysis rates in clean and polluted marine environments, J. Geophys. Res., 112, D21308, doi:10.1029/2007JD008442, 2007.
Köhler, H.: The nucleus in and the growth of hygroscopic droplets, T. Faraday Soc., 32(2), 1152–1161, 1936.
Langmuir, J.: The constitution and fundamental properties of solids and liquids – Part 1: Solids, J. Am. Chem. Soc., 38, 2221–2295, 1916.
Meskhidze, N., Nenes, A., Conant, W. C., and Seinfeld, J. H.: Evaluation of a new cloud droplet activation parameterization with in situ data from CRYSTAL-FACE and CSTRIPE, J. Geophys. Res., 110, D16202, doi:10.1029/2004JD005703, 2005.
Ming, Y., Ramaswamy, V., Donner, L. J., and Phillips, V. T. J.: A new parameterization of cloud droplet activation applicable to general circulation models, J. Atmos. Sci., 63, doi:10.1175/JAS3686.1, 2006.
Nenes, A., Ghan, S., Abdul-Razzak, H., Chuang, P. Y., and Seinfeld, J. H.: Kinetic Limitations on Cloud Droplet Formation and Impact on Cloud Albedo, Tellus B, 53, 133–149, 2001.
Nenes, A. and Seinfeld, J. H.: Parameterization of cloud droplet formation in global climate

models, J. Geophys. Res., 108, 4415, doi:10.1029/2002JD002911, 2003.
Nenes, A., Charlson, R. J., Facchini, M. C., Kulmala, M., Laaksonen, A., and Seinfeld, J. H.: Can chemical effects on cloud droplet number rival the first indirect effect?, Geophys. Res. Lett., 29(18), 1848, doi:10.1029/2002GL015295, 2002.
Peng, Y., Lohmann, U., and Leaitch, W. R.: Importance of vertical velocity variations in the cloud droplet nucleation process of marine stratocumulus, J. Geophys. Res., 110, D21213, doi:10.1029/2004JD004922, 2005.
Pontikis, C. A., Rigaud, A., and Hicks, E. M.: Entrainment and mixing as related to the microphysical properties of shallow warm cumulus clouds, J. Atmos. Sci., 44, 2150–2165, 1987.
Seinfeld, J. H. and Pandis, S. N.: Atmospheric Chemistry and Physics, John Wiley, New York, USA, 1998.
Seisel, S., Pashkova, A., Lian, Y., and Zellner, R.: Water uptake on mineral dust and soot: a fundamental view of hydrophilicity of atmospheric particles, Faraday Discuss., 130, 437–451, 2005.
Sorjamaa, R. and Laaksonen, R.: The effect of H_2O adsorption on cloud-drop activation of insoluble particles – a theoretical framework, Atmos. Chem. Phys., 7, 6175–6180, 2007, http://www.atmos-chem-phys.net/7/6175/2007/.
Twomey, S.: Pollution and the Planetary Albedo, Atmos. Environ., 8, 1251–1256, 1974.
Wexler, A. S. and Ge, Z. Z.: Hydrophobic particles can activate at lower relative humidity than slightly hygroscopic ones: A Köhler theory incorporating surface fixed charge, J. Geophys. Res., 103, 6083–6088, 1998.
Whitby, K. T.: The physical characteristics of sulphur aerosols, Atmos. Environ., 12, 135–139, 1978.
Wiegner, M., Gasteiger, J., Kandler, K., Weinzierl, B., Rasp, K., Esselborn, M., Freudenthaler, V., Heese, B., Toledano, C., Tesche, M., and Althausen, D.: Numerical simulations of optical properties of Saharan dust aerosols with emphasis on linear depolarization ratio, Tellus B, in press, 2008.

Table 1. Comparison of critical to dry particle diameter for FHH and Köhler particles.

D_{dry} (μm)	$(D_c/D_{dry})_{FHH}$ [a]	$(D_c/D_{dry})^{b}_{Köhler}$
0.01	1.81	3.13
0.025	1.86	4.80
0.05	1.91	7.00
0.075	1.93	8.53
1.00	2.13	31.31
2.50	2.23	49.48
5.00	2.30	70.01
7.50	2.32	85.75
10.00	2.38	99.02
15.00	2.44	121.27
20.00	2.48	140.03

[a] D_c calculated from Eq. (6), A_{FHH}=0.68, B_{FHH}=0.93, D_w=2.75 A°

[b] D_c calculated from Eq. (8), ν=3, σ=0.72 N m^{-1}, M_w=0.018 kg mol^{-1}, M_w=132.14 g mol^{-1}, ρ_w=1000 kg m^{-3}

ACPD
8, 16851–16890, 2008

Table 2. Fitting parameters for $D_{j,i}$ in Eq. (21).

$D_{j,i}$	j=1	j=2	j=3	j=4	j=5
i=1	−0.1907	−1.6929	1.4963	−0.5644	0.0711
i=2	−3.9310	7.0906	−5.3436	1.8025	−0.2131
i=3	8.4825	−14.9297	11.4552	−3.9115	0.4647
i=4	−5.1774	8.8725	−6.8527	2.3514	−0.2799

ACPD
8, 16851–16890, 2008

Table 3. Cloud formation conditions considered in this study.

Property	Values
α_c	0.042, 0.06, 1.0
V ($m\,s^{-1}$)	0.1, 0.5, 1.0, 5.0, 10.0
T_{parcel} (K)	298
P_{parcel}(Pa)	9×10^5
(A_{FHH} , B_{FHH}) combinations considered for FHH particles	(0.25, 2.00), (0.50, 1.75), (0.50, 1.00), (0.68, 0.93), (0.75, 2.00) (0.85, 1.00), (1.00, 2.00), (1.50, 1.50), (2.00, 1.00), (2.00, 2.50)

ACPD
8, 16851–16890, 2008

Table 4. Aerosol lognormal size distributions used in this study for Köhler particles (Whitby, 1978).

	Nuclei Mode			Accumulation Mode			Coarse Mode		
Aerosol Type	D_{g1}	σ_1	N_1	D_{g2}	σ_2	N_2	D_{g3}	σ_3	N_3
Marine	0.010	1.6	340	0.070	2.0	60	0.62	2.7	3.1
Continental	0.016	1.6	1000	0.068	2.1	800	0.92	2.2	0.72
Background	0.016	1.7	6400	0.076	2.0	2300	1.02	2.16	3.2
Urban	0.014	1.8	106000	0.054	2.16	32000	0.86	2.21	5.4

D_{gi} is the median diameter (μm), N_i is the number of dry particles (cm^{-3}), and σ_i is the geometric standard deviation of the ith mode. Each particle was assumed to contain 50% soluble $(NH_4)_2SO_4$ and 50% insoluble material by mass.

Table 5. Aerosol lognormal size distributions used in this study for FHH particles that are representative of mineral dust aerosol (see Jeong and Sokolik, 2007).

	Mode 1			Mode 2			Mode 3			Mode 4		
Size Distribution	D_{g1}	σ_1	MF_1%	D_{g2}	σ_2	MF_2%	D_{g3}	σ_3	MF_3%	D_{g4}	σ_4	MF_4%
C04 (Clarke et al., 2004)	0.69	1.46	1.8	1.77	1.85	69.4	8.67	1.50	28.8	–	–	–
D87 (D'Almeida, 1987)	0.16	2.10	1.0	1.40	1.90	95.3	9.98	1.60	3.7	–	–	–
O98 (Hess et al., 1998)	0.14	1.95	3.4	0.78	2.00	76.1	3.80	2.15	20.5	–	–	–
W08 (Weigner et al., 2008)	0.078	2.2	2.93	0.495	1.7	0.81	1.40	1.9	31.53	6.50	1.7	64.73

D_{gi} is the median diameter (μm), σ_i is the geometric standard deviation, and MF_i% is the percentage mass fraction of dry particles of the ith mode. Particle number concentration was calculated from percentage mass fraction by assuming a total mass equal to 4000 μg m^{-3} and particle density equal to 2.5 g cm^{-3} in the first three distributions. For Weigner et al. (2008), number concentration was converted to percentage mass fraction of dry particles in each mode. Each particle was assumed to contain 50% soluble $(NH_4)_2SO_4$ and 50% insoluble material by mass.

ACPD
8, 16851–16890, 2008

Table 6. Droplet number agreement between the parameterization and parcel model, for each aerosol type and conditions in Table 3.

Aerosol Type	Relative Error	(%) Standard Deviation
Whitby Background (Whitby, 1978)	+5	±12
Whitby Marine (Whitby, 1978)	−20	±10
Whitby Continental (Whitby, 1978)	+2	±6
Whitby Urban (Whitby, 1978)	+7	±17
D87 (D'Almeida, 1987)	+8	±12
O98 (Hess et al., 1998)	+2	±15
W08 (Weigner et al., 2008)	+4.5	±25

ACPD
8, 16851–16890, 2008

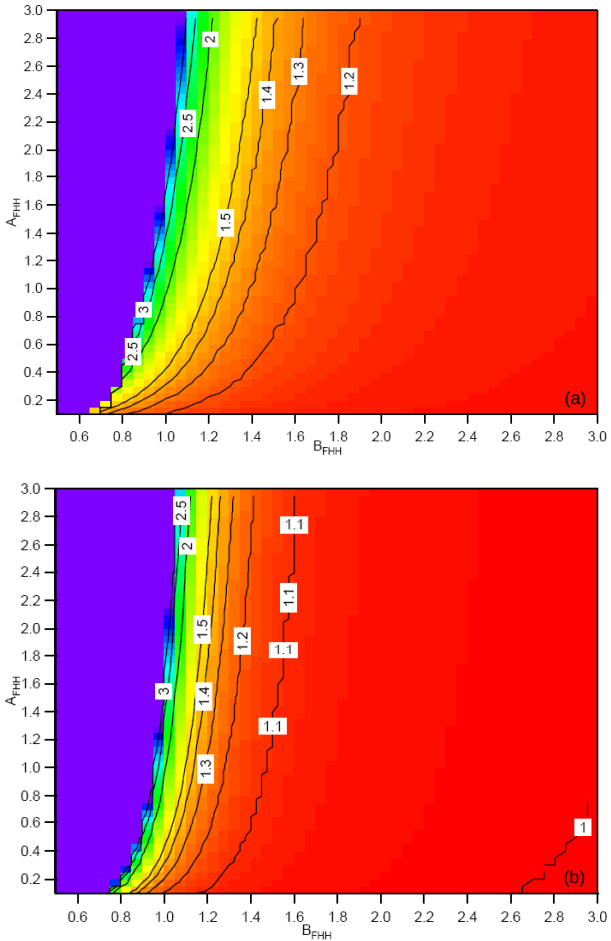

Fig. 1. D_c/D_{dry} contours as a function of A_{FHH} and B_{FHH} for **(a)** D_{dry}=0.25 μm, and **(b)** D_{dry}=20 μm.

ACPD
8, 16851–16890, 2008

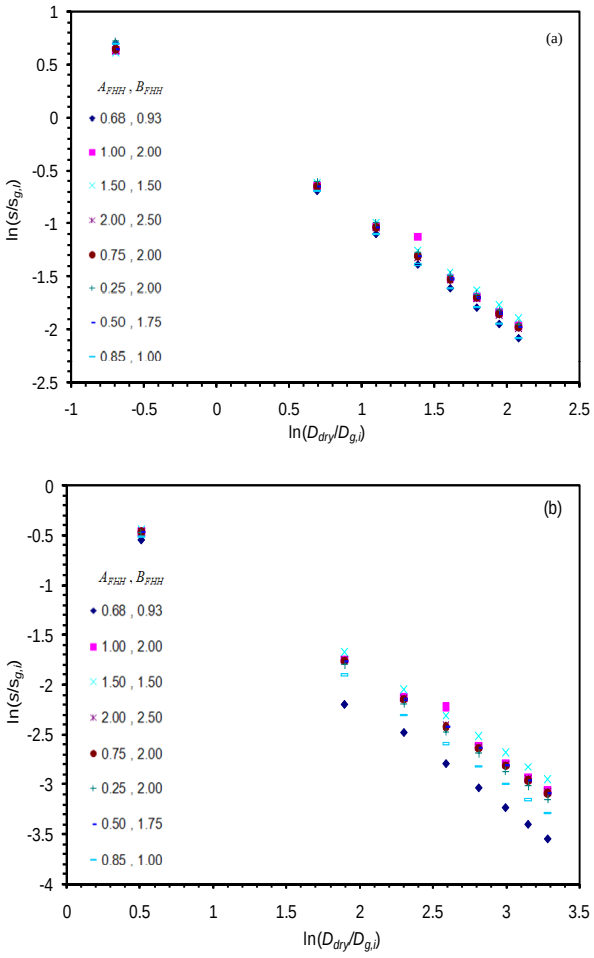

Fig. 2. Plot of $\ln(s/s_{g,i})$ vs. $\ln(D_{\mathrm{dry}}/D_{g,i})$ for **(a)** $D_{g,i}$=0.1 μm, and **(b)** $D_{g,i}$=0.03 μm.

ACPD
8, 16851–16890, 2008

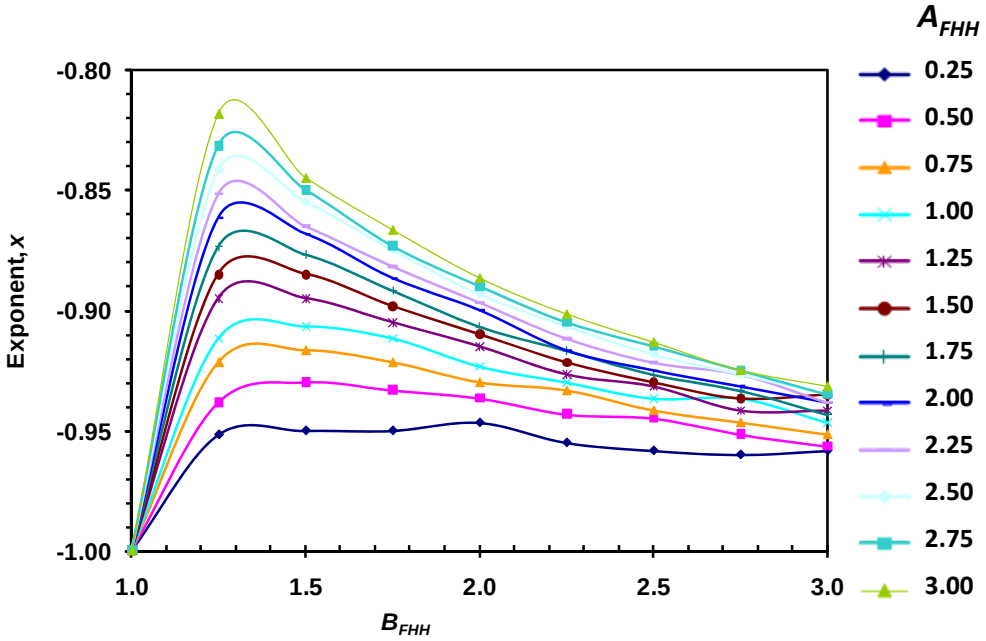

Fig. 3. Exponent x for FHH particles as a function of B_{FHH} for different values of A_{FHH}.

ACPD
8, 16851–16890, 2008

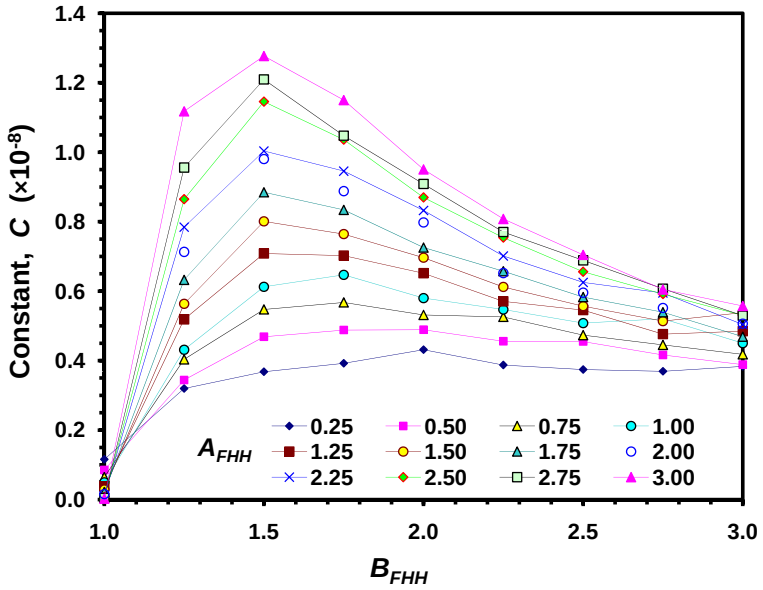

Fig. 4. Constant C (m^{-x}), which relates s_c of FHH particles to D_{dry} as $s_c = CD_{dry}^{x}$. C is presented for the range of B_{FHH} and A_{FHH} in which insoluble particles can act as CCN.

ACPD
8, 16851–16890, 2008

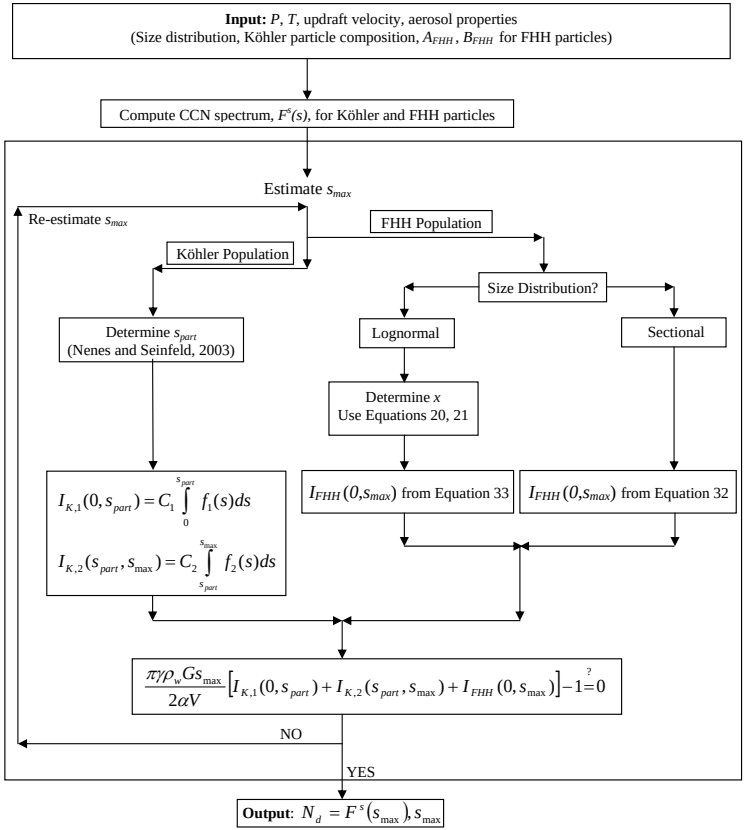

Fig. 5. Parameterization Algorithm. C_1, C_2, $f_1(s)$, $f_2(s)$ depend on the aerosol representation (sectional, lognormal) and are defined in Nenes and Seinfeld (2003).

ACPD
8, 16851–16890, 2008

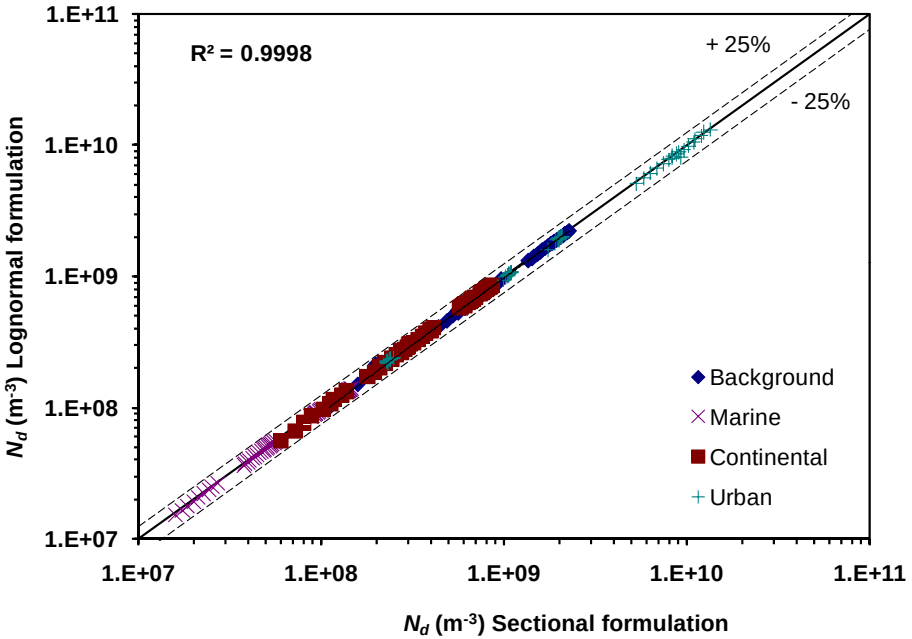

Fig. 6. Droplet number concentration, N_d (m^{-3}), predicted by the sectional and the lognormal formulations for Whitby (1978) distributions and for the cloud formation conditions of Table 3. Results are shown for α_c=0.042, and A_{FHH}=0.68 and B_{FHH}=0.93. 75 sections were used to discretize the lognormal distribution. Dashed lines represent ±25% deviation.

ACPD
8, 16851–16890, 2008

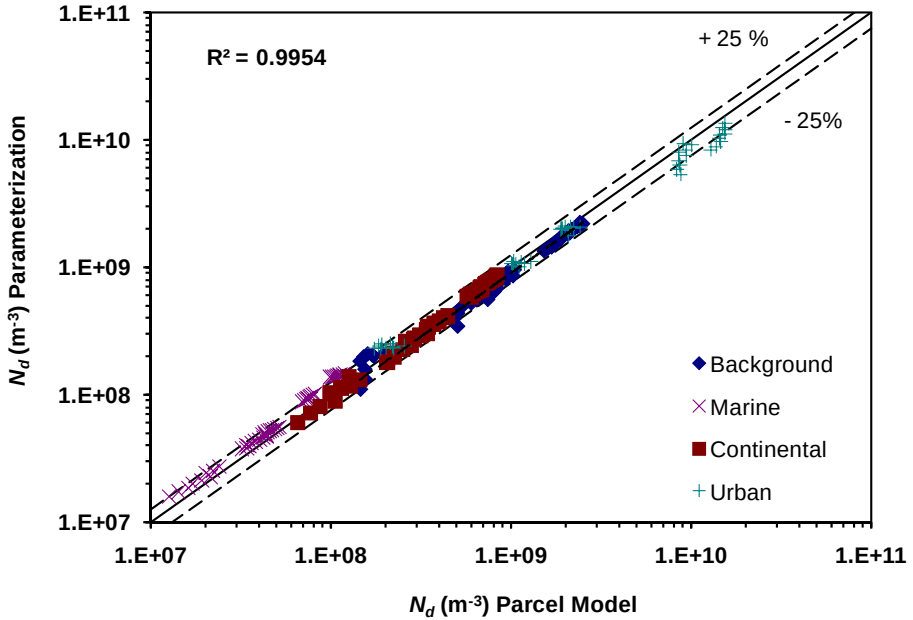

Fig. 7. Droplet number concentration, N_d (m^{-3}), predicted by parameterization and the parcel model for Whitby (1978) distributions, for the cloud formation conditions of Table 3. Results are shown for α_c=0.042, and A_{FHH}=0.68 and B_{FHH}=0.93. Dashed lines represent ±25% deviation.

ACPD
8, 16851–16890, 2008

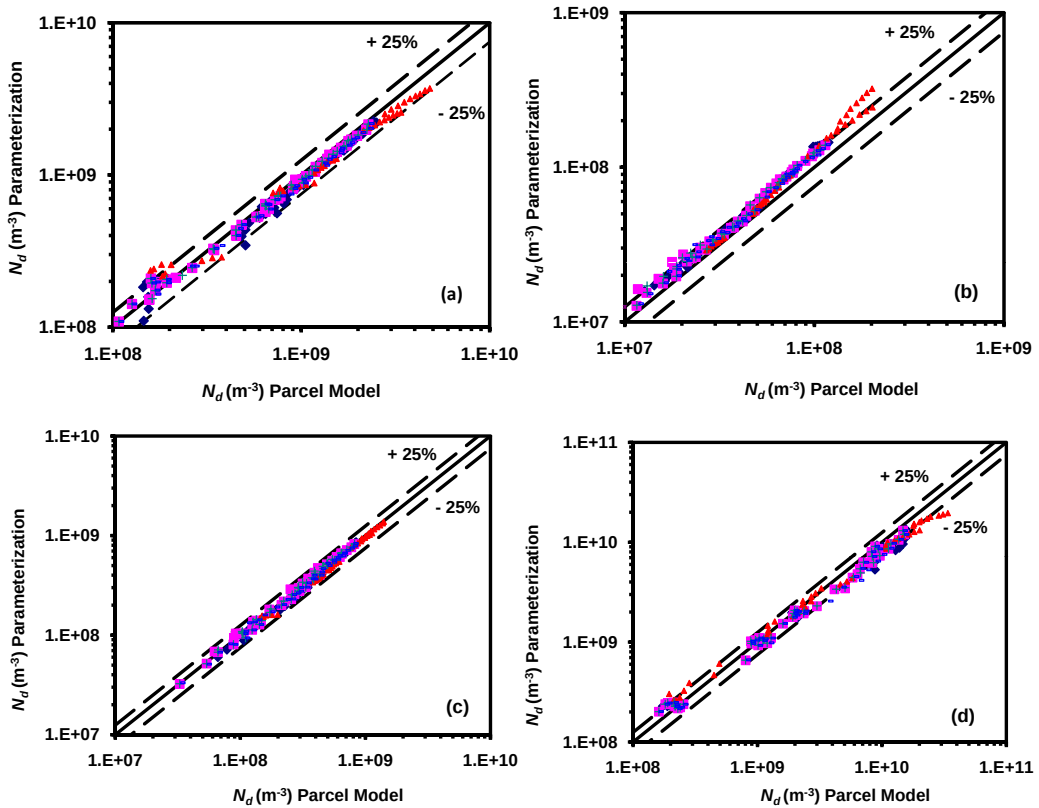

Fig. 8. Droplet number concentration, N_d (m^{-3}), predicted by parameterization and the parcel model for Whitby (1978) distributions, **(a)** Background, **(b)** Marine, **(c)** Continental, and **(d)** Urban, for the cloud formation conditions of Table 3. Results are shown for α_c=0.042 and ♦ A_{FHH}=0.68, B_{FHH}=0.93; ■ A_{FHH}=2.00, B_{FHH}=2.50; ▲ A_{FHH}=2.00, B_{FHH}=1.00; + A_{FHH}=0.50, B_{FHH}=1.75; – A_{FHH}=1.50, B_{FHH}=1.50. Dashed lines represent ±25% deviation.

ACPD
8, 16851–16890, 2008

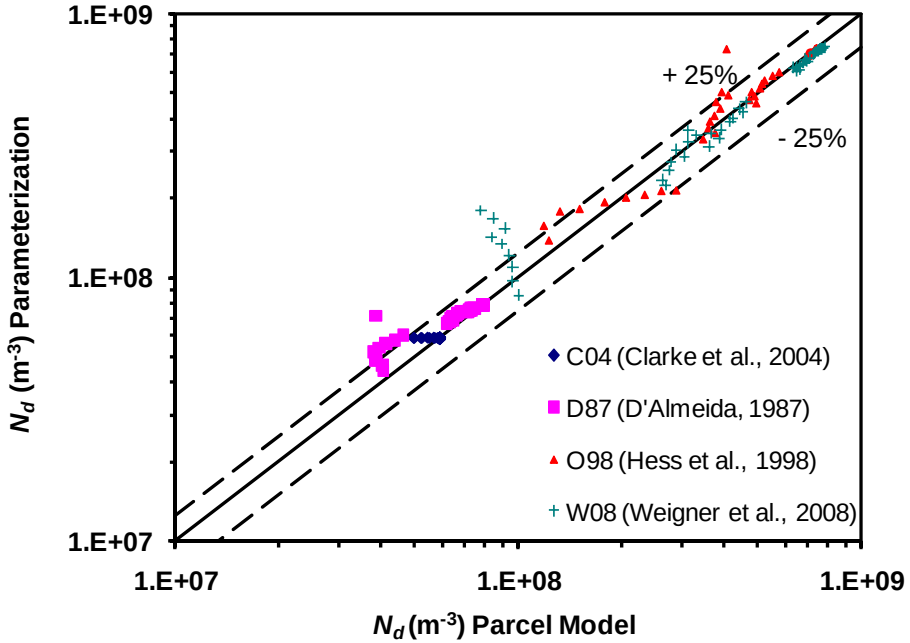

Fig. 9. Droplet number concentration, N_d (m^{-3}), predicted by the parameterization and the parcel model for dust size distributions (see Table 5), for the cloud formation conditions of Table 3. Results are shown for α_c=0.042, and A_{FHH}=0.68 and B_{FHH}=0.93. Dashed lines represent ±25% deviation.

ACPD
8, 16851–16890, 2008

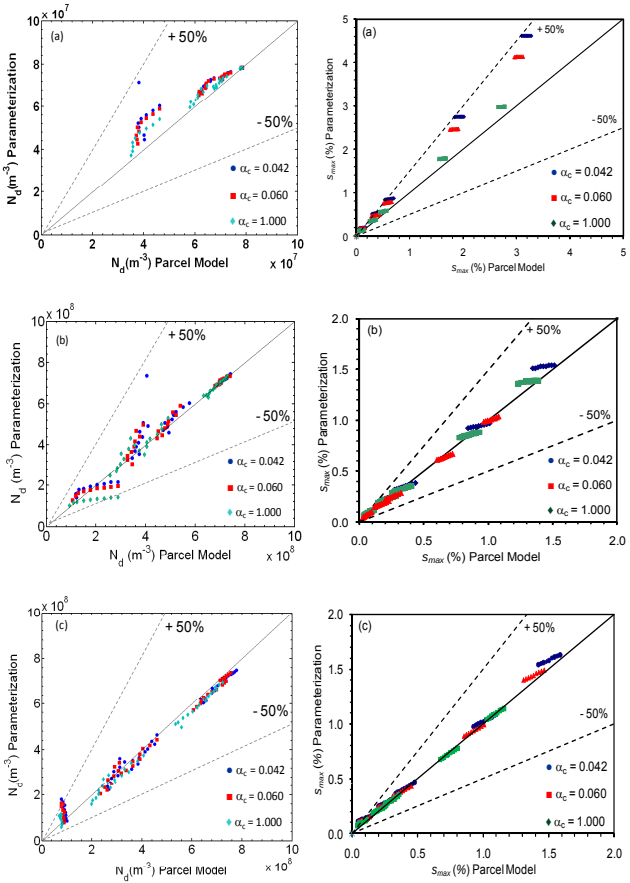

Fig. 10. Droplet number concentration, N_d (left panels) and parcel maximum supersaturation, s_{max} (right panels), predicted by the parameterization and the parcel model, for the V, α_c conditions of Table 3, and dust size distributions of **(a)** D'Almeida (1987), **(b)** Hess et al. (1998) and, **(c)** Weigner et al. (2008) for A_{FHH}=0.68 and B_{FHH}=0.93 in all simulations.

ACPD
8, 16851–16890, 2008